ELSEVIER

Polymer 44 (2003) 2711–2719

polymer

www.elsevier.com/locate/polymer

Phase separation of diamine chain-extended poly(urethane) copolymers: FTIR spectroscopy and phase transitions

James T. Garrett[1], Ruijian Xu[2], Jaedong Cho[3], James Runt*

Department of Materials Science and Engineering and Materials Research Institute The Pennsylvania State University, University Park, PA 16802, USA

Received 6 November 2002; received in revised form 6 February 2003; accepted 11 February 2003

Abstract

As part of our continuing effort to understand microphase separation of poly(urethane urea) block copolymers, FTIR spectroscopy and thermal techniques (DSC and DMA) were used to investigate the phase behavior of two series of MDI–polytetramethylene oxide soft segment copolymers, chain-extended with ethylene diamine or a diamine mixture. Due to the complex nature and multiple absorbances in the carbonyl and N–H regions of the FTIR spectra, quantitative analysis was not possible. However, qualitative trends could be discerned, and the spectral changes were found to be in excellent agreement with our previous quantitative analysis of the same copolymers using small-angle X-ray scattering. DSC and DMA experiments both indicate that the soft phase T_g decreases with increasing hard segment content. This is contrary to increased hard segment mixing in the soft phase, but can be rationalized by taking into consideration soft segment crystallinity and the concentration of 'lone' MDI units in the soft phase.
© 2003 Elsevier Science Ltd. All rights reserved.

Keywords: Polyurethane; Phase separation; Phase transitions

1. Introduction

Segmented polyurethane block copolymers are regularly used in cardiac surgery, e.g. as intraaortic balloons, in catheters, and as blood sacs and other components in cardiac assist devices [1]. There are also a number of fully implantable medical devices on the horizon that make significant use of multiblock polyurethanes as blood-contacting materials: e.g. the Arrow LionHeart ventricular assist device and the Abiomed AbioCor total artificial heart. The design of polymeric materials for these applications is a challenging problem. For example, the material used to construct the blood sacs in the pumping chamber of the latter devices must be elastomeric, have outstanding flexural fatigue characteristics, as well as good biocompatibility. In addition, the polymer must be amenable to processing into complex shapes and have low permeability to water and gases. The permeability issue is an important one if the patient is to be self-sufficient, and some of our recent research has addressed this topic [2,3].

Diamine chain-extended polyurethanes [i.e. poly(urethane urea)s] are of particular interest in biomedical applications. It is well established that such copolymers usually phase separate into high T_g (sometimes crystalline) 'hard' domains and relatively low T_g 'soft' domains, on cooling from the melt or precipitation from solution [4–7]. The degree to which the hard and soft segments microphase separate and the resulting morphology have a profound effect on the copolymer's ultimate properties. Despite their importance, there is, in general, inadequate understanding of hard segment–soft segment phase separation and the influence of thermal and process history on phase separation in these materials.

2. Background

We embarked a few years ago on the study of the nanoscale morphology and intersegment mixing of two series of segmented polyurethane copolymers (termed

* Corresponding author. Tel.: +1-814-863-2749; fax: +1-814-865-2917.
E-mail address: runt@matse.psu.edu (J. Runt).
[1] Present address: Chemistry Division, Naval Research Laboratory, Washington, DC, USA.
[2] Present address: Johns Manville, Littleton, CO, USA.
[3] Present address: POSCO Technical Research Laboratories, Korea.

0032-3861/03/$ - see front matter © 2003 Elsevier Science Ltd. All rights reserved.
doi:10.1016/S0032-3861(03)00165-4

Series I and II throughout this article, see the next section) prepared using a 2000 g/mol poly(tetramethylene oxide) [PTMO], end-capped with 4,4′-methylene di(*p*-phenyl isocyanate) [MDI], and chain extended with ethylene diamine [EDA] or a diamine mixture [EDA and 1,-4 diamino cyclohexane (DACH)]. The phase separated morphology of these materials was characterized by tapping mode atomic force microscopy (AFM) [8]. Phase images of free surfaces of films (cast from DMAc) of all Series I and II copolymers exhibit both randomly oriented cylinders and domains that appear more or less spherical. The hard domains have lateral dimensions on the order of 5–10 nm, and the lengths of the cylinders can exceed 100 nm. The widths of the hard domains are comparable to the average sizes reported for other solution cast segmented polyurethanes from AFM and transmission electron microscopy experiments [9,10].

A second group of AFM experiments was conducted on slightly thicker cast films of the Series I and II polymers, that had been ultracryotomed or freeze-fractured through their cross-section at low temperatures. Hard domains are apparent at low tapping forces in the cross-sections, in comparison to images of free surfaces, presumably because of the absence of a soft phase overlayer. Many of the hard domains seen in the cross-section of the copolymers were approximately spherical in shape, while others are modestly elongated. The two-dimensional power spectral densities of a cross-sectional image of a selected copolymer (having 22 wt% hard segments) yielded an average interdomain spacing of ~12 nm, in good agreement with an interdomain spacing of 13 nm derived from small-angle X-ray scattering (SAXS) experiments on the identical copolymer. At higher hard segment contents (i.e. ≥30 wt% hard segment) larger structures are observed in AFM phase images, which upon imaging at low tapping forces are seen to be aggregates of the smaller hard domains.

The domain morphology of the copolymers can be clearly characterized in the AFM experiments, but they do not provide insight into how efficiently the hard and soft segments are phase separated. For this we turned to SAXS experiments [11,12]. Since the Series I and II copolymers clearly exhibit a non-lamellar morphology, we used a general approach to analyze the SAXS data, that nevertheless permits quantification of overall degrees of phase separation, the influence of interfacial boundaries, and mixing of unlike segments in the hard and soft domains. This approach involves measuring the scattering invariant (determined from the total scattered intensity) and using this to calculate experimental electron density variances. The experimental variances are then compared to a calculated (theoretical) variance for the case of complete hard segment–soft segment separation. The details of these calculations and the overall approach are summarized in Refs. [11,13,14].

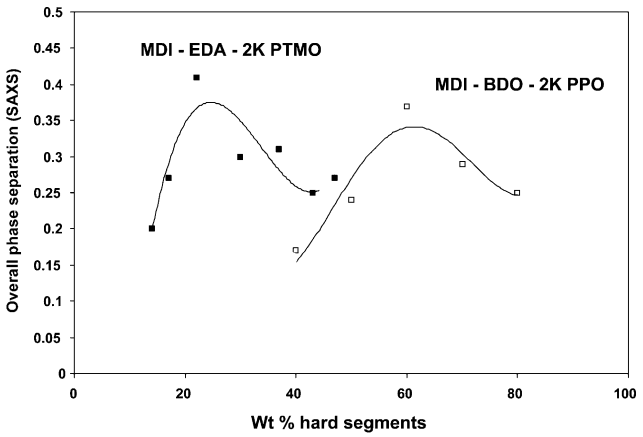

Fig. 1. SAXS degrees of phase separation for MDI–EDA–2K PTMO copolymers used in this study (filled symbols) and MDI–BDO–2K PPO copolymers (open symbols) from Ref. [14]. The curves through the two data sets were drawn simply to guide the eye, and are not meant to imply a particular functional form.

Below ~22% hard segment content, overall degrees of phase separation[4] of the Series I copolymers increase with increasing hard segment content, as shown in Fig. 1. This supports the idea of a critical hard segment sequence length, above which hard segments reside in hard domains, and below which they are dissolved in the soft phase [15]. However, for the higher hard segment content Series I copolymers, the overall degrees of phase separation are significantly reduced. This behavior arises from the non-equilibrium condition of the higher hard segment content materials, as verified in annealing experiments [12]. It is of interest to compare the degrees of phase separation for these diamine chain-extended copolymers with comparable diol [i.e. ethanediol] chain-extended materials. However, the only other similar series of data that appears in the literature are for copolymers prepared from MDI, butanediol (BDO) and a 2000 molecular weight polypropylene oxide macrodiol [14]. Nevertheless, the phase separation values for these copolymers are also plotted in Fig. 1. The diamine chain-extended copolymers generally exhibit greater degrees of phase separation at comparable hard segment contents, although the kinetic effects noted above are important in limiting demixing for copolymers having only 30 wt% hard segments. A similar restriction in demixing is observed for the MDI/BDO/PPO copolymers, although this sets in at higher hard segment contents.

Common poly(urethane urea)s are not truly thermoplastic since they cannot be melt processed due to soft phase degradation at temperatures below the hard domain glass transition or melting temperature. As a result, components of medical devices made from these materials must be manufactured by casting the polymer from solution.

[4] The 'overall degrees of phase separation' as determined by this approach are based on the total number of hard and soft segments. One cannot distinguish between mixing of hard segments in soft domains and vice versa using this method.

Consequently, we previously explored the role of the solution casting process, and subsequent thermal history, on the phase separated morphology and segment intermixing in the domains [12].

In summary, microphase separation of segmented polyurethanes is probably the single most influential characteristic of these materials. The degree of phase separation plays a key role in determining mechanical properties [15–17] and, apparently, blood compatibility [18], both vital in biomedical applications. Phase separation in multiblock polyurethane copolymers has been studied by a variety of techniques that approach the problem from different perspectives. In the present study, we augment our earlier AFM and SAXS studies with a parallel investigation of hydrogen bonding characteristics via Fourier Transform Infrared (FTIR) spectroscopy and of the various transition temperatures and transition enthalpies. We conclude with a brief discussion of hard domain order.

3. Experimental

3.1. Poly(urethane urea) copolymers

The synthesis of the two series of diamine chain-extended polyurethanes used in the present study was described in a previous publication [11]. The molecular weight distributions, relative to poly(ethylene oxide) standards, were determined using gel permeation chromatography. Dimethylformamide–0.05 M lithium bromide at 80 °C was used as the mobile phase. The apparent weight average molecular weights and polydispersity indices for all copolymers are provided in Table 1.

The copolymers used in the present research are identical to those used in our previous studies [8,11,12]. EDA alone was used as the chain extender in the first group of copolymers, referred to as Series I. The Series I copolymers are identified by 'PUU' and a number denoting the hard segment weight fraction (calculated by assigning all MDI and EDA units to the hard segment). All copolymers in Series II have the same hard segment weight fraction (0.22), but a portion of the EDA was replaced with DACH such that the relative molar ratio of EDA as the chain extender varied from 1 to 0.65. The second diamine was incorporated in order to partially disrupt hydrogen bonding in the hard phase. In designating the Series II copolymers, the hard segment weight fraction appears first, followed by the percentage of total diamine that is DACH.

Table 1
Series I and II poly(urethane urea) copolymers

	% DACH	M_w g/mol	M_w/M_n
Series I			
PUU 14	–	50,900	1.6
PUU 17	–	81,400	2.2
PUU 22	–	47,800	2.0
PUU 30	–	33,300	2.3
PUU 37	–	37,900	2.7
PUU 43	–	20,800	2.5
PUU 47	–	14,200	2.3
Series II			
PUU 22	0	47,800	2.0
PUU 22-5	5	39,800	1.9
PUU 22-15	15	46,000	2.3
PUU 22-25	25	57,600	2.1
PUU 22-35	35	76,300	3.0

3.2. Characterization

3.2.1. Fourier transform infrared spectroscopy

Several drops of ~3 wt% solutions of the copolymers in DMAc were placed on polished KBr windows with a disposable pipette. These samples were then dried in an oven at 70 °C under vacuum. If necessary, the amount of polymer solution was adjusted to yield films of an appropriate thickness required to stay within the range of Beer's Law. FTIR experiments were conducted on a Biorad FTS 45 spectrometer. Each sample was scanned 64 times at a resolution of 2 cm^{-1} and the scans were signal averaged.

3.2.2. Differential scanning calorimetry

Differential scanning calorimetry (DSC) evaluation of all samples was conducted using a Seiko DSC 220 CU equipped with a liquid nitrogen cooling accessory. Samples were first cooled to −130 °C then heated to 150 °C at a rate of 10 °C/min. After holding at 150 °C for 10 min the samples were cooled again to −130 °C and finally heated to either 280 or 300 °C at the rate of 10 °C/min.

3.2.3. Dynamic mechanical analysis (DMA)

Samples for DMA experiments were cut from films cast under identical conditions as those used in previous studies. Samples were cut to 10 mm × 40 mm, and the thickness of the films measured with a micrometer. Multiple thickness measurements were averaged and were generally on the order of 200 μm.

Storage (E') and loss moduli as a function of temperature were measured using a Polymer Laboratories Dynamic Mechanical Thermal Analyzer in tensile mode. A temperature programmer was connected to a liquid nitrogen delivery system. All samples were scanned from −130 to 200 °C at 3 °C/min and a frequency of 1 Hz. A constant force of 0.8 N was applied to all samples and maintained throughout the experiment.

3.2.4. Copolymer thermal stability

Thermogravimetric analysis experiments on the Series I and II copolymers indicate that they do not lose appreciable mass until 200 °C [19]. However, chemical degradation may of course occur in the absence of significant weight loss, and FTIR temperature studies were conducted to investigate this possibility. Changes in the spectra at higher temperatures [19]

are indicative of soft segment degradation. This is not particularly surprising in that polyethers are well known to be susceptible to oxidation and are degraded by attack from molecular oxygen and peroxides. The mechanism is via attack of the α methylene group and reaction to form C=O [20], decreasing the number of ether moieties while increasing the non-hydrogen bonded carbonyls. This process is detected at ~190 °C, about 50–60 °C lower than the traditional 2% weight loss marker in the TGA experiments.

In order to determine the maximum temperature to which the copolymers could be exposed without inducing oxidative degradation, a second series of FTIR temperature studies were conducted. FTIR spectra were acquired every 20 °C while samples were heated to a maximum temperature and subsequently cooled to room temperature. There were no discernible differences in any spectrum during heating to temperatures up to 150–170 °C and hence this is generally the maximum temperature samples were exposed to during any temperature excursion.

4. Results and discussion

4.1. Fourier transform infrared spectroscopy

4.1.1. Series I copolymers

There are two regions of the FTIR spectra of particular interest in the investigation of phase separation of segmented poly(urethane urea)s. The first is the carbonyl stretching region, which contains at least five separate bands and is located between ~1620 and 1760 cm^{-1}. This region is shown in Fig. 2 for selected Series I copolymers. The absorbance at 1636 cm^{-1} represents C=O groups that are hydrogen-bonded to urea N–H groups in a 'three-dimensional' hydrogen bond [21–23] where one C=O is hydrogen bonded to both N–H groups of a nearby urea moiety. This is conventionally referred to as an 'ordered' urea C=O, but does not necessarily indicate a crystalline hard domain. Urea C=O groups may also hydrogen bond to only one urea or urethane N–H, in a disordered fashion. This peak is located at 1666 cm^{-1}, while the non-hydrogen bonded urea C=O is located around 1700 cm^{-1} [23,24]. It seems likely that both contribute to the intensity between ~1710 and 1650 cm^{-1} in Fig. 2. The hydrogen-bonded and non-bonded urethane C=O are found at 1715 cm^{-1} and 1732 cm^{-1}, respectively [22,25]. Non-bonded carbonyls may not be completely 'free', as the corresponding N–H in the urethane linkage may be bonded to another carbonyl, or to an ether oxygen of the soft segment [24,26]. It has been proposed that the relative degree of microphase separation in amine chain-extended polyurethanes can be assessed by determining the degree of urea C=O hydrogen bonding [27], and that an increase in the extent of microphase separation is accompanied by an increase in absorbance of the ordered urea C=O peak [24].

Due to the number and relatively poor resolution of the bands in this region in Fig. 2, quantitative peak analysis is inappropriate. However, qualitative trends can be discerned. Each spectrum in Fig. 2 was first normalized using the area of the 1412 cm^{-1} peak, assigned to the C–C stretching mode of the aromatic ring [28]. This peak has been used previously [25,29] as a reference and its assignment is non-controversial. The spectra were adjusted so that the relative peak areas of the absorbance at 1412 cm^{-1} are the same as the calculated ratio of aromatic rings in the copolymers. A second series of normalizations was also conducted using the area of the peak at 821 cm^{-1} (associated with the C–H bending mode of the aromatic rings [25,29]) to confirm the scaling factors.

The second area of interest is the N–H stretching region, which is located between 3100 and 3500 cm^{-1} and shown in Fig. 3. The peak at 3320 cm^{-1} has been assigned to the stretching mode of hydrogen-bonded N–H in both urethane and urea units [25,29] In model polyureas, this peak was found to sharpen as the urea groups became ordered [23] Disordered, hydrogen-bonded N–H groups are characterized by absorbance near 3390 cm^{-1}, and the peak due to non-bonded N–H groups is located near 3450 cm^{-1} [23].

In Fig. 2, it is seen that the intensity of the ordered urea C=O peak increases with increasing hard segment content up to PUU 22, indicating a increase in hard–soft segment phase separation with increasing hard segment content. For

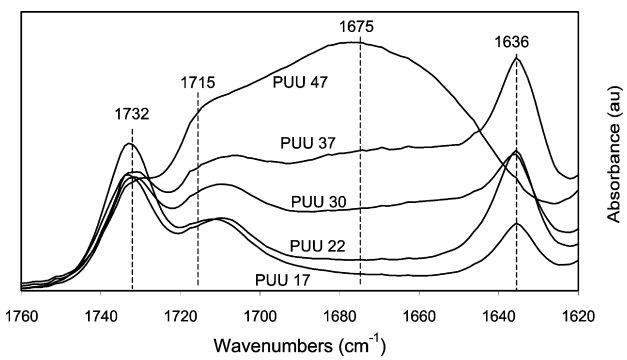

Fig. 2. FTIR spectra of selected Series I copolymers in the carbonyl stretching region.

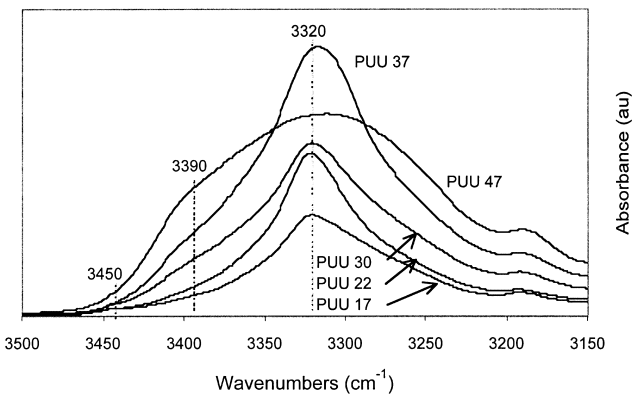

Fig. 3. N–H stretching region of FTIR spectra of selected Series I copolymers.

PUU 30, the intensity of the bonded urea C=O peak is approximately the same as that for PUU 22, but the absorbance in the region of the disordered and free urea C=O is significantly increased. A decrease in the ratio of the absorbance of the ordered peak at 1636 cm^{-1} to that of the disordered and free urea C=O suggests a decrease in hard segment–soft segment phase separation, compared to PUU 22. In the spectrum of PUU 37, the intensity of the urea peaks increases by approximately the same amount, indicating a degree of microphase separation on the same order as that of PUU 30. Finally, the peak associated with ordered urea carbonyls is virtually absent in the spectrum of PUU 47 and the relative intensity of the disordered and bonded urea C=O has increased significantly. Therefore, the ratio of ordered to disordered/free urea C=O is heavily in favor of the disordered/free carbonyls, indicative of even less phase separation than in PUU 30 and 37.

The N–H region of the spectra confirms these conclusions. The intensity at 3320 cm^{-1} increases with hard segment content for PUU 17 and 22, without significant intensity around 3390 cm^{-1}. The relatively sharp band at 3320 cm^{-1}, indicating ordered N–H, does not increase significantly from PUU 22 to PUU 30, but PUU 30 does exhibit broadening in this region. This implies an increase in disordered N–H in the absence of a corresponding increase in ordered N–H groups and is consistent with a decrease in phase separation. The shape of the absorbance in this region for PUU 37 (although of higher intensity) is similar to that of PUU 30 and only a broad peak is observed in this region for PUU 47. The peak shape for the latter is similar to that seen for an amorphous polyurea [23], which points to primarily disordered hard domains and lower phase separation for PUU 47, compared to PUU 30 and 37.

Finally, note the excellent agreement between the conclusions derived from the FTIR spectra, and those from the quantitative SAXS determination of overall degrees of phase separation [11] shown in Fig. 1.

4.1.2. Series II copolymers

The FTIR spectra of the C=O stretching region of selected Series II copolymers are shown in Fig. 4. Substitution of DACH for some of the EDA chain extender results in a significant reduction in hydrogen bonding in the hard domains. The intensity of the 1636 cm^{-1} band is significantly reduced, and some additional intensity is observed around 1700 cm^{-1}. This is consistent with a transition of bonded and ordered urea C=O to non-bonded C=O, and indicates that the addition of the second diamine causes a reduction in the degree of phase separation for copolymers with the same hard segment content. Again, these results are in excellent agreement with our previous SAXS determination of overall degrees of phase separation.

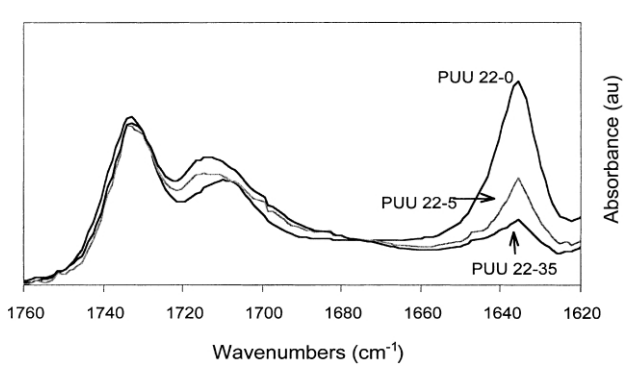

Fig. 4. FTIR spectra of selected Series II copolymers in the carbonyl stretching region.

4.2. Phase transitions

4.2.1. Series I copolymers

Representative thermograms for the Series I copolymers obtained on heating, after cooling to − 130 °C, are shown in Fig. 5. The arrows in the figure indicate the location of the soft phase glass transition temperature, $T_{g,s}$, which increases in breadth at higher hard segment contents. The T_gs and any T_ms of the hard domains could not be determined due to the onset of degradation at temperatures >150–170 °C. However, like others [5,30] we did observe an endotherm in the 270–290 °C temperature range for all Series I copolymers.

Particularly at lower hard segment contents, $T_{g,s}$ is followed by an exotherm, indicative of (additional) soft segment crystallization on heating. The melting endotherms associated with crystalline soft segments (crystallization occurs on cooling below ambient) are observed between 0 and 20 °C, with melting points ($T_{m,ss}$) increasing as hard segment content decreases. $T_{g,s}$ as well as $T_{m,ss}$ and the crystallinity of the soft segments are summarized in Table 2. The reported soft segment crystallinity has been normalized to the weight fraction of the soft segments in the copolymer, and calculated based on the heat of fusion of 100% crystalline PTMO, 201 J/g [31]. The decrease in crystallinity and $T_{m,ss}$ with increasing hard segment content is likely associated with increased mixing of hard segments in the soft domains, as shown by our SAXS experiments.

For higher hard segment content copolymers (PUU 43 and 47), a broad endotherm is observed between ~40 and 80 °C. For polyurethanes synthesized from diisocyanates and diols, a transition in this temperature range has been

Table 2
Soft phase T_gs, T_ms, and degrees of crystallinity for Series I copolymers

Sample	$T_{g,s}$ (°C)	$T_{m,ss}$ (°C)	Normalized soft segment crystallinity (%)
PTMO diol (2K)	−78	43	89
PUU 14	−64	16	26
PUU 17	−66	9	18
PUU 22	−67	4	18
PUU 30	−73	2	7
PUU 37	−74	1	6
PUU 43	−74	1	5
PUU 47	−77	0	4

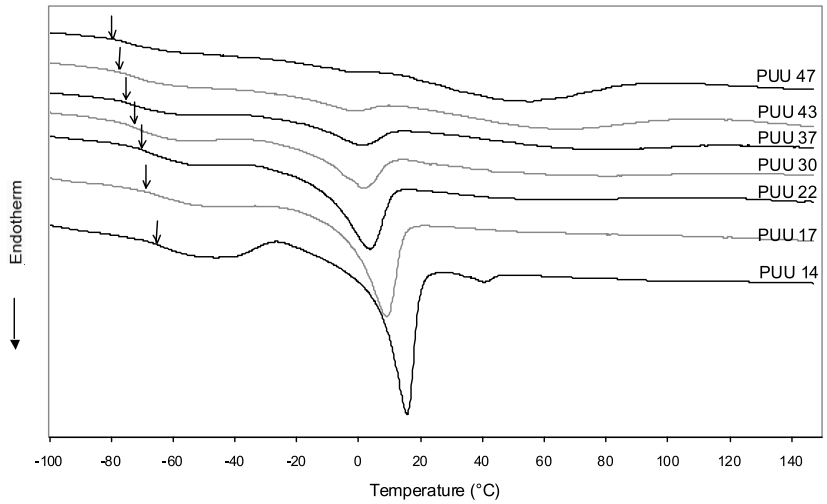

Fig. 5. DSC thermograms of the Series I copolymers.

assigned to the disruption of short-range order [32,33] or the hard domain T_g, $T_{g,h}$ [15,34] The origin of this transition in diamine chain-extended polyurethanes has only been investigated in one previous FTIR study. Ishihara et al. observed a decrease in the intensity of the hydrogen-bonded N–H absorbance (3320 cm^{-1}) as their poly(urethane urea) sample was heated to 100 °C, but observed no changes in the carbonyl stretching region [29]. Consequently, these authors argued that this was a result of disruption of N–H to ether–O–hydrogen bonds in the soft phase. However, FTIR spectra as a function of temperature of the Series I and II copolymers (not shown) display changes in both the C=O stretching and hydrogen-bonded N–H regions. Consequently, changes in N–H hydrogen bonding cannot be exclusively attributed to disruption of H-bonding in the soft phase.

The DMA storage modulus (E') is plotted as a function of temperature for the Series I copolymers in Fig. 6a. The corresponding tan δ–T plots are shown in Fig. 6b. In the glassy state, the storage moduli of all copolymers are on the order of $10^{9.5}$ Pa, a typical value for polymer glasses. There is a significant reduction in E' as the specimens pass through the α_a transition, which is associated with segmental motion in the soft phase [35,36]. A peak corresponding to the α_a transition is readily apparent in the tan δ–T plot, and the temperatures of these transitions are presented in Table 3. As expected, the location of the α_a transition follows the same trend with hard segment content as does $T_{g,s}$.

The α_a transition is followed by a further reduction in modulus near 0 °C, likely associated with the melting of the soft segments that crystallize on cooling to low temperatures prior to the DMA experiment. This transition generally presents itself as a shoulder on the high temperature side of the α_a peak in the tan δ curve. The strength of both the α_a and melting processes are dependent on copolymer content; the strength of the α_a transitions for copolymers higher in soft segment content are larger. For the higher hard segment content copolymers, a third transition is observed near ~150–180 °C, similar to data reported for other PTMO–MDI–EDA copolymers [5]. DSC studies on TDI–EDA [37] and MDI–EDA [38] polyurethanes have assigned a transition in this region (<200 °C) to $T_{g,h}$. However, another transition at an even higher temperature (>250 °C) has been observed. As noted earlier, our higher temperature DSC experiments reveal a similar endotherm above 250 °C, but due to polymer degradation in this temperature range the data are not presented here. This

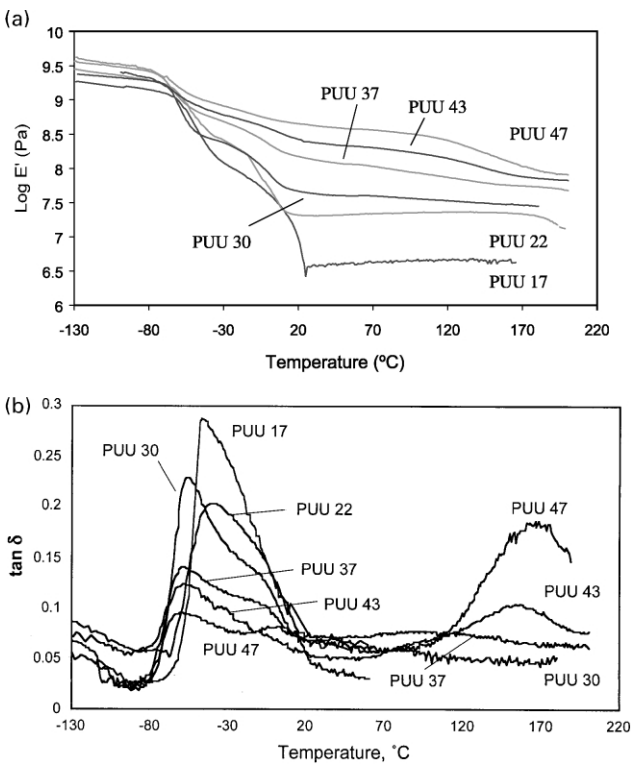

Fig. 6. (a) Storage modulus as function of temperature for the Series I copolymers; (b) tan δ as function of temperature for the Series I copolymers.

Table 3
$T_{\alpha,a}$ and plateau moduli for Series I and II copolymers

	$T_{\alpha,a}$ (°C)	Plateau modulus (Pa)
Series I		
PUU 17	−38	$10^{6.65}$
PUU 22	−42	$10^{7.35}$
PUU 30	−55	$10^{7.55}$
PUU 37	−57	$10^{7.93}$
PUU 43	−58	$10^{8.2}$
PUU 47	−59	$10^{8.45}$
Series II		
PUU 22-0	−42	$10^{7.35}$
PUU 22-5	−51	$10^{6.35}$
PUU 22-15	−53	$10^{6.64}$
PUU 22-25	−52	$10^{6.58}$
PUU 22-35	−52	$10^{6.56}$

highest temperature transition is most often assigned to the melting of crystalline hard domains [5] but has occasionally been associated with the hard domain T_g, and/or the dissociation of hard domain hydrogen bonding [30].

Finally, at temperatures above $T_{m,ss}$, E' remains relatively constant, and the average plateau moduli are presented in Table 3. log E' in the plateau region scales linearly with hard segment weight fraction, for copolymers covering the range of hard segment contents under investigation here.

The location of $T_{g,s}$ as well as the enthalpy and location of the soft segment melting endotherm are sometimes used as indicators of phase purity in multiblock polyurethanes. If the copolymer is assumed to behave like a blend of homopolymers, the T_g of the phases in the blend can be compared to those of the neat components to determine the degree of hard/soft segment mixing. In the case of MDI–EDA based polyurethanes, the T_gs of the hard domains are inaccessible but the experimental soft phase T_gs can be compared to that of the PTMO (2K) diol. As seen in Table 2, the T_gs of the soft phase *decrease* with increasing hard segment content. This has also been observed, although not emphasized, in other DSC studies of diamine chain-extended polyurethanes containing polyether [5,6,39] and polyester [37] soft segments. If one follows the simple argument advanced above, this would indicate that the soft phase is becoming enriched in PTMO as hard segment content increases. However, this is counter to intuition, as well as the results of the SAXS experiments on the identical copolymer samples.

The results of our previous SAXS studies show that intersegment mixing is indeed an important factor, and should be considered in the interpretation of $T_{g,s}$. Hard segments have a much higher T_g than the neat soft segment and the more hard segments trapped or dissolved in the soft phase, the higher the expected $T_{g,s}$. Following from interpretation of thermal analysis experiments on diol-based polyurethanes, it is reasonable to assume to a first approximation that the hard domains in the poly(urethane urea)s under investigation here are pure (i.e. consist of hard segments only) [14], and that shorter hard segment lengths are the first to be dissolved into the soft phase [40,41]. This being the case, the SAXS data indicate that the concentration of hard segments in the soft phase increases with increasing hard segment content. However, this argument is not consistent with the observed decrease in $T_{g,s}$ (or $T_{\alpha,a}$) with increasing hard segment content. Clearly, dissolved hard segments in the soft phase are *not* the primary factor determining soft phase T_g in the Series I copolymers.

There are several additional factors that need to be considered to explain the peculiar decrease in $T_{g,s}$ with increasing hard segment content. Soft segments are expected to be attached frequently to hard segments that have segregated into high T_g hard domains. This would lead to reduced mobility of at least a portion of such soft segments, raising the T_g. Although this argument is in keeping with the greater breadth of the T_g interval in the higher hard segment copolymers, it is contrary to the observed reduction in $T_{g,s}$ with increasing hard segment content.

The soft segment crystallinity that develops on cooling also must be considered. The introduction of, and increase in, crystallinity in polymers like poly(ethylene terephthalate) is well known to result in an increase in T_g, and this has been suggested for poly(urethane urea)s as well [6]. This is due to the restriction in mobility of amorphous units due to the anchoring of 'neighboring' segments by crystallites. Lower hard segment content Series I copolymers crystallize to a significantly higher extent (Table 2) and, if crystallinity is the factor dominating $T_{g,s}$, $T_{g,s}$ would be expected to decrease as hard segment content in the PUU increases. This is precisely what is observed experimentally, and agrees with previous arguments that soft phase crystallinity is more sensitive to phase composition than the soft phase T_g [18,38].

Finally, the concentration of 'lone MDIs' in the soft phase should be considered. A lone MDI occurs when both isocyanate groups of a single MDI unit react with PTMO macrodiols. This results in two PTMO chains joined in the absence of any urea groups. The lone MDI species are not expected to phase separate into hard domains, and contribute only in the soft phase. The insertion of lone MDI moieties into PTMO 'chains' would logically lead to an increase in $T_{g,s}$. In fact, in research on 1:1 copolymers of MDI and PTMO [42], it was inferred that such units can raise $T_{g,s}$ by 10 °C, similar to our observations in Table 2. Due to the statistical nature of the end-capping reaction, the lowest hard segment content copolymers are calculated [43] to have the highest concentration of lone MDIs, and considering only the effect of lone MDIs, they should have the highest $T_{g,s}$.

Finally, it is worth pointing out the nearly constant values of $T_{g,s}$ for copolymers ranging from 30 to 43 wt% hard segments. In light of the previous discussion, this is not surprising in that the degree of soft segment crystallinity and

calculated number of lone MDIs do not differ significantly between these materials.

In summary, as evidenced by the preceding discussion, the soft phase T_g of multiblock copolymers (particularly those for which the soft segment crystallizes on cooling below ambient) can be influenced by many factors. Great care must therefore be exercised when any attempt is made to 'back out' a soft phase composition from $T_{g,s}$, as is sometimes done in the literature. Such an analysis is clearly inappropriate for the copolymers under consideration here.

4.2.2. Series II copolymers

The DSC thermograms for the DACH containing copolymers (Fig. 7) are very similar to PUU 22, with the most noticeable difference being the larger crystallization exotherm near −25 °C. Soft segments in PUU 22 are able to crystallize more efficiently on cooling because there is less segment intermixing in PUU 22 than in the DACH containing copolymers [11]. The reduction in crystallinity is quantified in Table 4. The degree of soft segment crystallinity (based on the weight of PTMO in the copolymers) is significantly reduced for all copolymers containing DACH and is independent of DACH content.

PUU 22-15 and 22-35 also display endotherms similar to the higher hard segment content copolymers of Series I near 40–80 °C. Analogous to the argument advanced previously [29], additional intermixing in the DACH-containing polymers is likely to result in a relatively higher concentration of N–H to ether oxygen hydrogen bonds. The breaking of these bonds could contribute to the endotherm observed below 100 °C.

Storage moduli and tan δ vs. temperature for the Series II copolymers are shown in Fig. 8. There is a notable reduction in E' at temperatures above $T_{\alpha,a}$ for all copolymers containing mixed diamines. The drop in plateau modulus (Table 3) is indicative of a lower volume fraction of phase separated hard domains. This behavior is consistent with the findings from our SAXS experiments that demonstrate that DACH-containing copolymers exhibit a lower degree of phase separation than PUU 22 [11]. The decrease in overall phase separation also hampers soft segment crystallization (Table 3). This reduction in crystallinity could contribute to the decrease in $T_{\alpha,a}$ for the DACH-containing copolymers. The other difference in the log $E'-T$ behavior of the Series II copolymers is a small increase in E' between $T_{g,s}$ and $T_{m,ss}$ for the mixed diamine copolymers. The 'humps' in the E' curves are unusual, but have also been observed for another poly(urethane urea) [18] and most likely result from crystallization of soft segments in this temperature range.

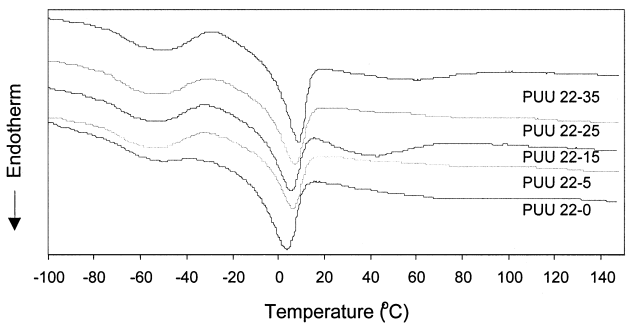

Fig. 7. DSC thermograms of the Series II copolymers.

Table 4
Soft phase $T_{g,s}$, $T_{m,ss}$ and normalized degree of crystallinity for Series II copolymers

Sample	$T_{g,s}$ (°C)	$T_{m,ss}$ (°C)	Soft segment crystallinity (%)
PUU 22	−67	4	18
PUU 22-5	−69	6	6
PUU 22-15	−68	6	5
PUU 22-25	−68	8	7
PUU 22-35	−66	9	8

5. Summary

The phase behavior of the Series I and II poly(urethane urea) copolymers has been investigated by a variety of experimental techniques, probing the structure from the

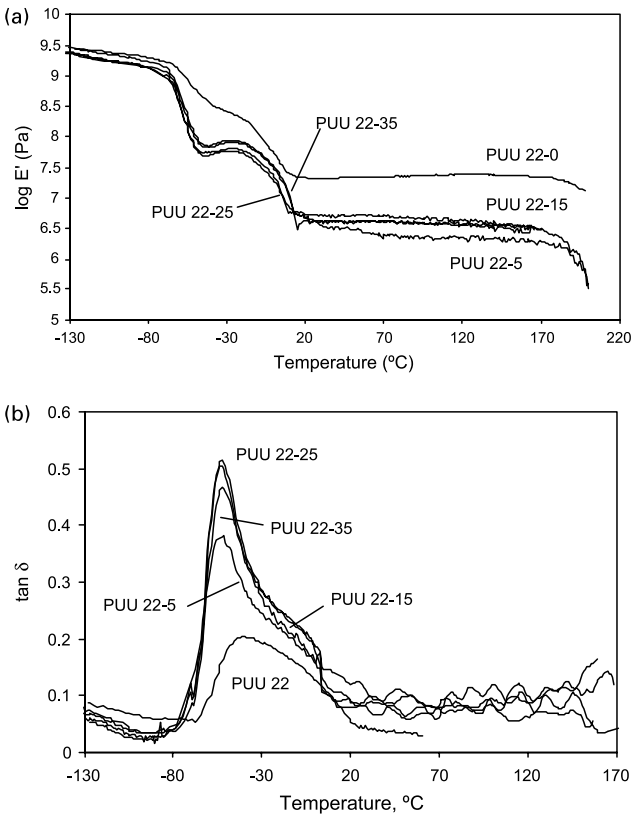

Fig. 8. (a) Storage modulus as a function of temperature for theSeries II copolymers; (b) δ as a function of temperature for the Series II copolymers.

molecular to the macroscopic levels, with all data pointing to the same conclusions. As hard segment content in the copolymers increases, phase separation increases up to the point where near 'equilibrium' demixing is unattainable due to kinetic restrictions on phase separation. For the Series I copolymers this sets in around ca. 25 wt% hard segments, but at ~60 wt% hard segments for MDI-BDO-2K PTMO copolymers [14]. At higher hard segment contents, unlike segment demixing is lower as the copolymers are trapped in a non-equilibrium condition. Despite the presence of hard segments in the soft phase, as demonstrated by SAXS and supported by FTIR experiments, the soft phase T_g was found to decrease with increasing hard segment content. Several factors can influence the soft phase T_g, but the two important ones for the Series I copolymers appear to be the crystallinity of the soft phase (formed on cooling to low temperatures) and the presence of 'lone' MDIs in the soft domain.

Finally, the addition of a second, larger diamine greatly inhibits phase separation, even when the second diamine constitutes only 5 mol% of the total diamine in the reaction. Urea hydrogen bonding is greatly reduced which leads to less phase separation (SAXS) and ultimately to reduced mechanical stiffness. By fully understanding the implications of copolymer chemistry and preparation techniques, this class of elastomers can be optimized to take full advantage of their inherent flexibility, durability, strength and blood compatibility.

Acknowledgements

We would like to express our appreciation to Prof. Michael Coleman (Penn State) and Dr Valeriy Ginzburg (Dow Chemical) for a number of helpful discussions. We would also like to thank Adam Roslund, Carolyn Avau and Talia Kleeb for their assistance with the DMTA, DSC and TGA experiments, respectively.

References

[1] Lamba NMK, Woodhouse KA, Cooper SL. Polyurethanes in biomedical applications. Boca Raton, FL: CRC Press; 1998.
[2] Weisberg DM, Gordon B, Rosenberg G, Snyder AJ, Benesi A, Runt J. Macromolecules 2000;33:4380.
[3] Xu R, Manias E, Snyder AJ, Runt J. Macromolecules 2001;34:337.
[4] Wilkes GL, Abouzahr S. Macromolecules 1981;14:458.
[5] Wang CB, Cooper SL. Macromolecules 1983;16:775.
[6] Sakurai S, Okamoto Y, Sakaue H, Nakamura T, Banda L, Nomura S. J Polym Sci Polym Phys 2000;38:1716.
[7] O'Sickey MJ, Lawrey BD, Wilkes GL. J Appl Polym Sci 2002;84:229.
[8] Garrett JT, Siedlecki CA, Runt J. Macromolecules 2001;34:7066.
[9] McLean RS, Sauer BB. Macromolecules 1997;30:8314.
[10] Li C, Cooper SL. Polymer 1990;31:3.
[11] Garrett JT, Runt J, Lin JS. Macromolecules 2000;33:6353.
[12] Garrett JT, Lin JS, Runt J. Macromolecules 2002;35:161.
[13] Bonart R, Müller EH. J Macromol Sci-Phys 1974;B10:345.
[14] Leung LM, Koberstein JT. J Polym Sci Polym Phys 1985;3:1883.
[15] Koberstein JT, Galambos AG, Leung LM. Macromolecules 1992;25:6195.
[16] Van Bogart JWC, Gibson PE, Cooper SL. J Polym Sci Polym Phys 1983;21:65.
[17] Christenson CP, Harthcock MA, Meadows MD, Spell HL, Howard WL, Creswick MW, Guerra RE, Turner RB. J Polym Sci Polym Phys 1986;24:1401.
[18] Takahara A, Tashita J, Kajiyama T, Takayanagi M, MacKnight WJ. Polymer 1985;26:978.
[19] Garrett JT. PhD Thesis, The Pennsylvania State University, 2001.
[20] Coleman MM, Yang X, Stallman JB, Painter PC. Macromol Symp 1995;94:1.
[21] Blackwell J, Nagarajan MR, Hoitink TB. Polymer 1982;23:950.
[22] Teo L-S, Chen C-Y, Kuo J-F. Macromolecules 1997;30:1793.
[23] Coleman MM, Sobkowiak M, Pehlert GH, Painter PC. Macromol Chem Phys 1997;198:117.
[24] Ning L, De-Ning W, Sheng-Kang Y. Macromolecules 1997;30:4405.
[25] McCarthy SJ, Meijs GF, Mitchell N, Gunatillake PA, Heath G, Brandwood A, Schindhelm K. Biomaterials 1997;18:1387.
[26] Coleman MM, Skrovanek DJ, Hu J, Painter PC. Macromolecules 1988;21:59.
[27] Bummer PM, Knutson K. Macromolecules 1990;23:4357.
[28] Srichatrapimuk VW, Cooper SL. J Macromol Sci Phys 1978;5:267.
[29] Ishihara H, Kimura I, Saito K, Ono H. J Macromol Sci Phys 1974;B10:591.
[30] Musselman SG, Santususso TM, Barnes JD, Sperling LH. J Polym Sci Polym Phys 1999;37:2586.
[31] Wunderlich B. Macromolecular physics. New York: Academic Press; 1973.
[32] Seymour RW, Cooper SL. Macromolecules 1973;6:48.
[33] Hesketh TP, Van Bogart JWC, Cooper SL. Polymer 1981;22.
[34] Chen TK, Shieh TS, Chui JY. Macromolecules 1998;31:1312.
[35] Shirasaka H, Inoue S, Asai K, Okamoto H. Macromolecules 2000;33:2776.
[36] Lelah MD, Lambrecht LK, Young BR, Cooper SL. J Biomed Mater Res 1983;17:1.
[37] Sung CSP, Hu CB, Wu CS. Macromolecules 1980;13:111.
[38] Hu CB, Ward RS, Schneider NS. J Appl Polym Sci 1982;27:2167.
[39] Lee HK, Ko SW. J Appl Polym Sci 1993;50:1269.
[40] Koberstein JT, Stein RS. J Polym Sci Polym Phys 1983;21:1439.
[41] Koberstein JT, Leung LM. Macromolecules 1992;25:6205.
[42] Lee DC, Register RA, Yang CZ, Cooper SL. Macromolecules 1988;21:1005.
[43] Peebles LH. Macromolecules 1976;9:58.